

## Oxidation Behavior of $\text{UO}_2$ in Air at 300~550°C

Kweon-Ho Kang, Suk-Youl Hwang\* and Kil-Jeong Kim

Korea Atomic Energy Research Institute, \*Pyeong Taek Technical College

**Abstract**—The oxidation behavior of  $\text{UO}_2$  pellets was studied using a thermogravimetric analyzer and an XRD in the temperature range of 300 to 550°C in air. From XRD studies it is found that  $\text{UO}_2$  is converted to  $\text{U}_3\text{O}_8$  and the weight gains of  $\text{UO}_2$  specimen are characterized by S-shape curves. After complete oxidation the specimens broke into fine powder and the average weight gain was about 3.93 wt%. The activation energy of 50% conversion of  $\text{UO}_2$  to  $\text{U}_3\text{O}_8$  is 81.6 kJ/mol and the oxidation rate per unit time was found to be as follows  $dw/dt=6.54 \times 10^6 e^{\frac{-81.6 \text{ kJ/mol}}{RT}}$ , wt%/h : at 50% conversion of  $\text{UO}_2$  into  $\text{U}_3\text{O}_8$  where  $w$ ,  $t$  and  $T$  were wt% gain, conversion time and temperature, respectively.

### 1. Introduction

A knowledge of the oxidation behavior of  $\text{UO}_2$  is necessary for evaluation of its stability in long-term storage and the disposal of spent fuels. There have been many studies on the oxidation of  $\text{UO}_2$ .<sup>1-9</sup> Aronson *et al.*<sup>1</sup> reported on the oxidation of  $\text{UO}_2$  powder that at temperatures below 260°C,  $\text{UO}_2$  was oxidized up to  $\text{UO}_2\cdot x$ , while above 260°C  $\text{UO}_2$  was oxidized up to  $\text{U}_3\text{O}_8$  by a two-step reaction through the phase  $\text{U}_2\text{O}_7$ . Peakall *et al.*<sup>2</sup> carried out the oxidation experiment for  $\text{UO}_2$  pellets in air at 350~1000°C. Scott *et al.*<sup>3</sup> carried out the oxidation for various uranium dioxide preparations in air at temperatures up to 800°C. Matae Iwasaki *et al.*<sup>4</sup> studied the oxidation of  $\text{UO}_2$  pellets in air at 800 and 900°C. They reported that there were three types of oxidation in the oxidation-time curve in temperature ranges from 400 to 700°C, 800 to 900°C and 900 to 1000°C. Matae Iwasaki *et al.*<sup>5</sup> carried out oxidation experiments for  $\text{UO}_2$  pellets in air at 400~700°C to investigate the effect of different heat treatment conditions of pellets on the particle size of the product of pulverization. Peter *et al.*<sup>6</sup> studied the early stages of  $\text{U}_3\text{O}_8$  formation on unirradiated CANDU  $\text{UO}_2$  fuel oxidized in air 200~300°C by using XRD. They reported that the XRD measurements permitted detection of  $\text{U}_3\text{O}_8$  formation earlier than the visual detection of the powder and  $\text{U}_3\text{O}_8$  was formed more ra-

pidly on a rough  $\text{UO}_2$  surface than a polished one. Bae *et al.*<sup>7</sup> studied the oxidation behavior of unirradiated  $\text{UO}_2$  pellets at 400 to characterize the oxidized powder and to establish a new spallation model. You *et al.*<sup>8</sup> studied the oxidation behavior of  $\text{UO}_2$  in the range of 250~400°C. They carried out the experiment on irradiated and non-irradiated  $\text{UO}_2$  and compared the two. Ritchie<sup>9</sup> reviewed reactions of uranium with oxygen and water vapor under various conditions.

In this paper the oxidation behavior of  $\text{UO}_2$  was studied and presented by XRD and thermogravimetry in the temperature range of 300~550°C in air for evaluating the stability of spent fuel in long-term storage and its disposal. The oxidation behavior of  $\text{UO}_2$  is compared with those of  $\text{UO}_2$  and metallic uranium previously reported by other studies.

### 2. Experimental Procedures

#### 2-1. Materials

Specimens having a dimension of 10.75 mm in diameter and 1.45~1.55 mm in thickness were cut from the commercial PWR type  $\text{UO}_2$  pellet whose nominal density is around 97% of theoretical density and grain size is about 10  $\mu\text{m}$ . It was made by sintering at 1,700°C in  $\text{H}_2$  after compacted under 12 bar pressure and its density was changed from 3.5  $\text{g/cm}^3$  to 10.7  $\text{g/cm}^3$ . The initial average weight and

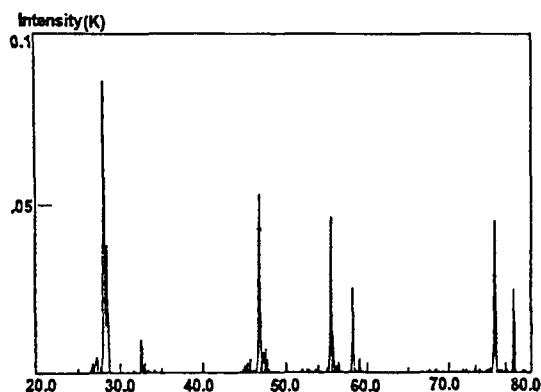


Fig. 1. XRD pattern of initial specimen.

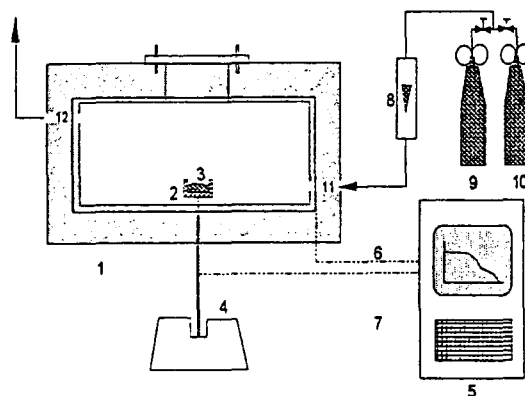
surface area of a specimen was 1,492  $\text{mm}^2$  and 232.2  $\text{mm}^2$ , respectively. Before tested, specimens were abraded with 600 grit silicon-carbide paper, washed in acetone in an ultrasonic cleaner, and rinsed with ethyl alcohol. All the specimens were stored in a dry environment and were tested with their surfaces covered with oxide films formed in air at room temperature. Fig. 1 shows a XRD pattern of the specimen before the oxidation experiment.

## 2-2. Apparatus

The experimental apparatus (thermogravimetric analyzing device) mainly consists of a furnace, a control and data acquisition system and a controlling system for the furnace. A schematic diagram of the thermogravimetric furnace is shown in Fig. 2. Temperature of the furnace can be controlled with any mode of heating by a programmable microprocessor. In order to avoid any reaction between the specimen and the crucible, an alumina crucible was used.

## 2-3. Experimental Procedure

The specimens were contained in the alumina crucibles to retain the non-adherent products and were brought to the test temperature in a flow of purified argon before the oxidant was introduced. The oxidation tests were performed by continuously weighing the samples in a stream of oxidizing gas. The weight gains of specimens were measured during the oxidation test by microbalance with a load-carrying capacity of 5 g and sensitivity of 1  $\mu\text{g}$ . Data



1. Furnace      2. Crucible      3. Sample  
4. Balance      5. Computer      6. Temp. Control  
7. Wt. Record      8. Flow Regulator      9. Argon Canister  
10. Oxygen Canister      11. Gas Inlet      12. Gas Outlet

Fig. 2. A schematic diagram of thermogravimetric furnace.

were automatically acquired and stored with the time and temperature. The flow rate of the oxidizing gas was 4.5  $\text{l/min}$  at an atmospheric pressure.

## 3. Results and Discussion

### 3-1. Oxidation Reaction and XRD Patterns

Fig. 3, 4 show the shape of specimens and XRD results after oxidation, respectively. When  $\text{UO}_2$  is oxidized in air, it can be transformed into various meta-stable oxides, such as  $\text{U}_3\text{O}_8$ ,  $\text{U}_4\text{O}_{11}$ , and  $\text{U}_2\text{O}_7$ . It is known that specimens of uranium dioxide after

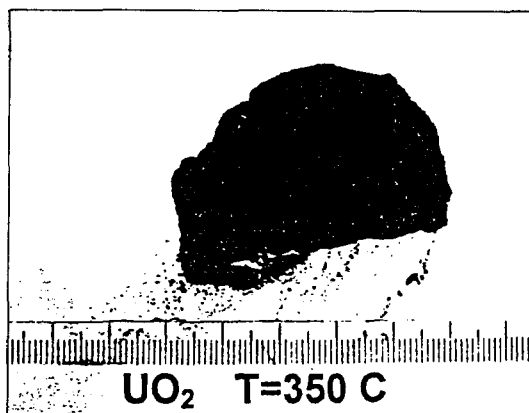


Fig. 3. Shape of the specimen after oxidation at 350°C for 500 min.

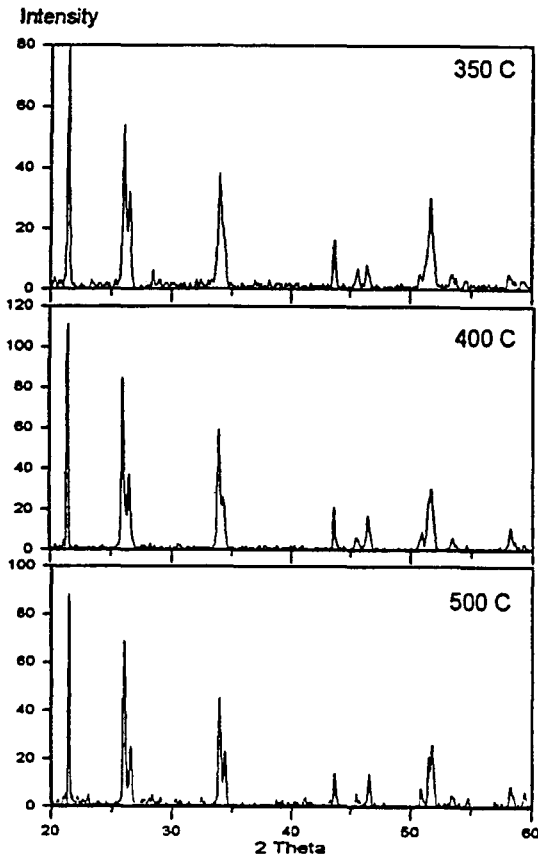


Fig. 4. XRD patterns of products after oxidation.

oxidation are fragmented and pulverized to powder due to the volume change resulting from phase transformation of  $\text{UO}_2$  to intermediate phases and finally  $\text{U}_3\text{O}_8$ . Aronson *et al.*<sup>11</sup> carried out the oxidation experiment with  $\text{UO}_2$  powder in air and oxygen at the temperature range of 160 to 350°C. They reported that the oxidation process could be divided into two steps. In the first step, the tetragonal oxide,  $\text{UO}_{2.34-0.03}$  is formed. In the second step, this tetragonal phase is converted to orthorhombic  $\text{U}_3\text{O}_8$ . In the oxidation of pelletized  $\text{UO}_2$ , Peakall *et al.*<sup>20</sup> reported that, at temperature range of 350 to 600°C, pellets were oxidized rather quickly to  $\text{U}_3\text{O}_8$  and were broken into fine particles. Scott *et al.*<sup>21</sup> reported that fine uranium dioxide powders were oxidized in the characteristically two step processes, first, to a tetragonal phase of the composition  $\text{UO}_{2.35-0.02}$  and then to  $\text{U}_3\text{O}_8$ . They also reported that uranium dioxide of low surface area was oxidized by only single stage

oxidation from  $\text{UO}_2$  to  $\text{U}_3\text{O}_8$ . Matae Iwasaki *et al.*<sup>41</sup> reported in their study for air-oxidation of  $\text{UO}_2$  pellets at 800 and 900°C that the oxidation of  $\text{UO}_2$  pellets proceeded by two steps: the first step,  $\text{UO}_2 \rightarrow (\text{UO}_{2.3}) \rightarrow \text{U}_3\text{O}_8$ , and the second step,  $\text{U}_3\text{O}_8 \rightarrow \text{U}_3\text{O}_{10}$ . The first step reaction proceeded from the surface into the inner layers of the pellets, and the reaction rate appeared to be controlled by the diffusion of oxygen through the  $\text{U}_3\text{O}_8$  phase. The second step reaction which proceeded rapidly with fragmentation of the pellet into small pieces, seems to be initiated by nucleation of  $\text{U}_3\text{O}_{10}$  in the  $\text{U}_3\text{O}_8$  phase. Bae *et al.*<sup>22</sup> reported that, as oxidation started at 400°C, the grain boundary was cracked because of the volume contraction and partial spallation of intermediate phases. During the oxidation intergranular cracks propagated towards the inside of the pellet and the formation of  $\text{U}_3\text{O}_8$  accelerated the spallation. In this study, the specimens were fragmented into fine powders followed by converting to  $\text{U}_3\text{O}_8$  in the range of temperature from 300 to 550°C. This result is different from the form of a well defined plate that is found in the oxidation of metallic uranium<sup>10</sup>.

### 3-2. Oxidation Rates

The oxidation rates of uranium and its alloys are various. They could be linear, parabolic or parabolic depending on the oxidation conditions. The factors that effect oxidation rate include temperature, moisture content, impurity, oxygen potential, roughness of surface, surface area vs. volume ratio, irradiation induced swelling, etc. Fig. 5 shows oxidation data obtained in this study over the temperature range of 300~550°C.

Aronson *et al.*<sup>11</sup> reported on the oxidation of  $\text{UO}_2$  powder that the rate controlling process in the first stage was the diffusion of oxygen through the uranium dioxide lattice. The value found as the diffusion coefficient  $D$  was expressed by,  $D=5.5 \times 10^{-11} \exp[(109,960 \pm 6,276)/RT]$ , where the activation energy was  $109.96 \pm 6.276$  kJ/mole. You *et al.*<sup>23</sup>, reporting on the oxidation behavior of  $\text{UO}_2$  in air, stated that the weight gain of the non-irradiated  $\text{UO}_2$  was characterized by the S-shape curve. In this study, the oxidation of  $\text{UO}_2$  proceeds slowly at the

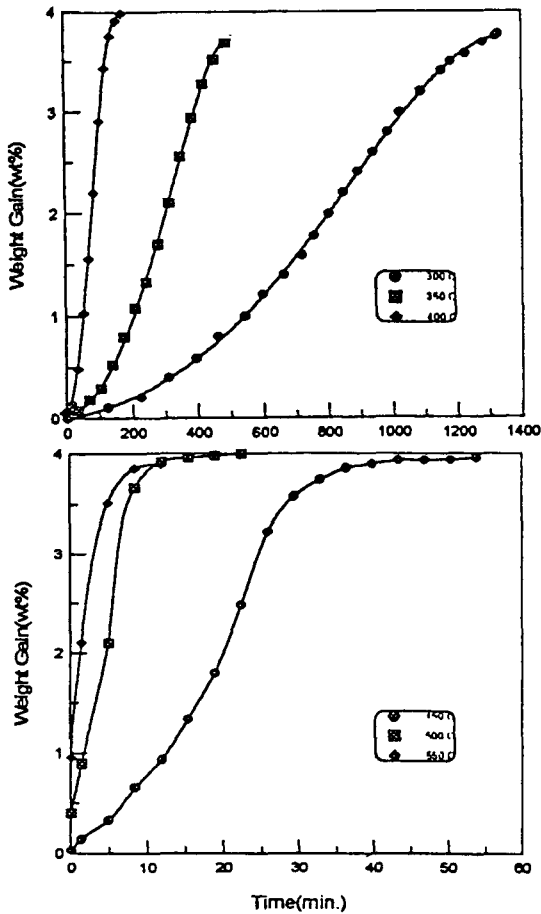


Fig. 5. Weight gain-time curves for the oxidation in air at 300–550°C.

initial stage of reaction and increases more sharply after a certain time until decreasing again due to slow reaction at the end of experiment. Therefore, the profile of the weight gain-time curve for this temperature range becomes S-shape, which is similar to the results of other studies. The S-shape profile of the weight gain-time curve is different from that obtained by a linear or parabolic reaction in the oxidation of metallic uranium<sup>8,10</sup>. The surface reaction could be controlled by the diffusion of oxygen into the internal structure of the specimen in the temperature range. Since the fragmentation of the specimen is caused by the volume expansion and the resulting powder increases the surface area for reaction, the reaction rate increases at higher orders at a certain period of time as explained pre-

Table 1. Oxidation rates of UO<sub>2</sub> with air.

Temp.	rate of oxidation, wt%/h		
	25% conversion	50% conversion	You <i>et al.</i> study
300	0.07	0.12	0.06
325			0.24
350	0.28	0.39	1.09
375			2.17
400	1.23	1.47	5.263
450	4.54	5.75	
500	8.41	25.8	
550	19.7	90.4	

viously. This observation supports the fact that the oxidation reaction process is controlled by diffusion of oxygen into the surface of the solid phase rather than the chemical reaction kinetics as one of the typical phenomena of the solid-gas reaction.

From the stoichiometric calculation of complete oxidation to U<sub>3</sub>O<sub>8</sub>, the weight gain of the final product would be to be 3.95 wt%. In this study, the weight gain of the final product is about 3.93 wt%. To observe the reaction rate of UO<sub>2</sub> with variation, the reaction rates at the gains of 25% and 50% are shown in Table 1.

The weight gain per unit time for 50% transformation vs. the reciprocal of the temperature is plotted and shown in Fig. 6. From an Arrhenius type expression for the rate equation, the activation energy were for weight gain of 50% were calculated

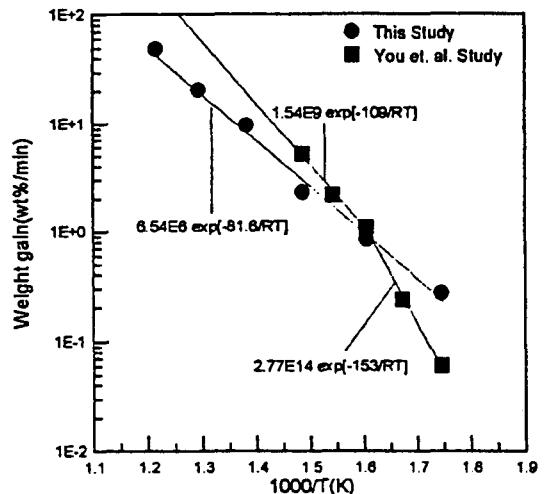


Fig. 6. Rate of weight gain versus 1000/T.

to be 81.6 kJ/mol in the range of 300~550°C, which is smaller than the value obtained by You *et al.*. You *et al.*<sup>9</sup> obtained the activation energies of 153 kJ/mol in 250~350°C and 110 kJ/mol in the range of 350~400°C. They also suggested the existence of a transition point at 350°C. In this study, however, the transition point did not appear. The activation energy is 81.6 kJ/mol. Because the oxidation was carried out in blowing air in this study but in You's study was carried out in stationary air, the oxygen potential was higher in this study than in You's study. In this study, from the plot, the reaction rate per unit time could be expressed as follows:

$$dw/dt = 6.54 \times 10^6 e^{\left(\frac{-81.6 \text{ kJ/mol}}{RT}\right)}, \text{ wt\%/h}$$

: at 50% transformation into U<sub>3</sub>O<sub>8</sub>

where the activation energy is 110.79 kJ/mol.

#### 4. Conclusions

Analyses of XRD patterns and thermogravimetry to observe the oxidation behavior of UO<sub>2</sub> pellet were carried out and the following conclusions could be made.

- 1) From XRD study, UO<sub>2</sub> pellet converted to U<sub>3</sub>O<sub>8</sub> in the temperature range of 300~550°C.
- 2) From thermogravimetry analysis, the weight gains of UO<sub>2</sub> specimens were characterized by S-shape curves.
- 3) The activation energy for 50% conversion of

UO<sub>2</sub> to U<sub>3</sub>O<sub>8</sub> was 81.6 kJ/mol and the oxidation rate per unit time was found to be:

$$dw/dt = 6.54 \times 10^6 e^{\left(\frac{-81.6 \text{ kJ/mol}}{RT}\right)}, \text{ wt\%/h}$$

: at 50% conversion of UO<sub>2</sub> into U<sub>3</sub>O<sub>8</sub>, where w, t and T were wt% gain, conversion time and temperature

4) After complete oxidation, the specimens were fragmented into fine powder.

#### Reference

1. Arosen, R.B. Roof, J.R. and J. Belle: *J. Chem. Phys.* **27**, 137 (1957).
2. K.A. Peakall and J.E. Antill: *J. Nucl. Mater.* **2**, 194 (1960).
3. K.T. Scott and K.T. Harrison: *J. Nucl. Mater.* **8**, 307 (1963).
4. Matae Iwasaki and Niro Ishikawa: *J. Nucl. Mater.* **36**, 116 (1970).
5. Matae Iwasaki, Tsutomu Sakurai and Niro Ishikawa: *J. Nucl. Sci. Tech.*, **5**, 652 (1968).
6. Peter T. Donald D. Wood and A. Michael Duclos: *J. Nucl. Mater.* **189**, 116 (1992).
7. K.K. Bae, B.G. Kim, Y.W. Lee, M.S. Yang and H.S. Park: *J. Nucl. Mater.* **209**, 274 (1994).
8. G.S. You, K.S. Kim, D.K. Min, S.G. Ro and E.K. Kim: *J. of KNS* **27**, 67 (1995).
9. A.G. Ritchie: *J. Nucl. Mater.* **102**, 170 (1981).
10. L. Baker, J.R. and J.D. Bingle, *J. Nucl. Mater.* **20**, 11 (1966).
11. M.J. Bennett, B.L. Myatt and J.E. Antill: *J. Nucl. Mater.* **50**, 2 (1974).